Solution Drying and Phase Separation Morphology of Polyacrylamide/Poly(ethylene glycol)/Water System

Karine Huraux, Tetsuharu Narita,* Christian Frétigny, and François Lequeux

PPMD UPMC-ESPCI-CNRS UMR7615, 10 rue Vauquelin, 75231 Paris Cedex 05, France

Received July 11, 2007; Revised Manuscript Received August 30, 2007

ABSTRACT: Blends of two immiscible polymers dissolved in a common solvent exhibit phase separation during drying of the solvent. This leads to different morphologies depending on the physical and physicochemical conditions of the systems. Here we report the final morphology of blend films of a glassy polymer (polyacrylamide, PAAm) and a crystalline polymer (poly(ethylene glycol), PEG) in water, prepared by blade coating with a controlled thickness from several to hundreds of micrometers. By changing the blend composition, we observed the inversion in morphology from mounds to holes via multiscale phase separation. A systematic study of PAAm-rich films having a morphology with holes revealed that two regimes may be distinguished depending on the drying rate: a heterogeneous drying regime where a glassy skin of PAAm is formed at the surface and fixes the morphology and a slow homogeneous drying regime where coalescence of holes is observed. Formation of monolayer of PEG crystals having fingerlike branched patterns at the surface of the PAAm matrix at different drying conditions is discussed.

Introduction

Phase separation in immiscible polymer blend films has been widely studied in recent decades. The blends which consist of two immiscible polymers dissolved in a common solvent exhibit phase separation when the solvent concentration reaches a critical value. This leads to different morphologies depending on the physical and physicochemical conditions of the systems such as solvent quality, chemical composition of the blends, film thickness, evaporation rate, and substrate nature. The surface structures of the films are of great interest from a technological point of view, since understanding and controlling the film morphology are important in a wide range of applications from biotechnology to microelectronics, for instance.

In previous studies, attention has been given both to the final morphology of the dried film and to the mechanisms and kinetics of the phase separation during drying. It was shown that the composition and the compatibility of the blends[1,2] and the solvent quality[3] have an effect on the length scale of surface morphologies by changing both the roughness and the homogeneity of the films. The thickness was also determined to have an effect on the morphology as it may modify chains conformation, interaction parameters, or degree of entanglement.[4]

Also, environmental parameters have been studied. An essential one is the evaporation rate which may be controlled by an excess vapor pressure. It was shown by laser confocal fluorescence microscopy that it influences both surface and bulk morphology.[5,6] The study of substrate[3,7] reveals a dependence of morphologies with the wetting properties of the surface and surface tensions.

As for the mechanisms, several phenomena[8] have been showed to occur during drying, leading to different final morphologies: gravitational sedimentation which leads to a droplets surface morphology, whereas in the bulk droplets sediment and coalesce,[9] inhomogeneous volatility, Bénard−Marangoni convections,[10] and the surface phase separation[11] divided into three distinct stages: the induction period when no phase separation is observed, the early stage when fast growth rate occurs, and the late stage when the domain size grows following a power-law relationship with time.

Here we report the final morphology of blend films of a glassy polymer (polyacrylamide, PAAm) and a crystalline polymer (poly(ethylene glycol), PEG) in water. The effects of the crystallization on the morphology are of interest, since the crystallization might lead to different morphologies compared with glassy polymers blends. Mishra and Rao reported the surface morphology of the poly(vinyl alcohol)/PEG/water system.[12] Although they observed different morphologies depending on the blend composition, a further systematic study is required to understand the effects of drying conditions. The system might attract attention as a model to study polymer crystallization, since the crystallization is affected by the interactions with substrates and the dimension of the system (the film thickness as well as the droplets size[13]). Unlike the previous works on either the surface morphology of very thin spin-coated films or the drying behavior of cast films (about 100 μm thick), we studied the final morphology of films obtained by blade coating which provide films with a controlled thickness from several to hundreds of micrometers. Moreover, we used water as solvent which entailed a very slow and easy to control drying phenomenon in comparison with organic solvents with low ebullition point.

By changing the blend composition, we observed the inversion in morphology due to phase separation between PAAm and PEG. Then we did a systematic study in order to discuss the effect of drying rate by changing two parameters in the experimental setup: the thickness of the film and the humidity.

Experimental Section

Materials. The polyacrylamide (PAAm, M_w = 600K−1000K, I_p = 11, T_g = 178 °C) and poly(ethylene glycol) (PEG, M_w = 35 000, I_p = 1.1, melting point 71 °C) were purchased from Polysciences Inc. (Warrington, PA). Ethanol and acetone were purchased from SDS (France). All the products were used as received. We used ultrapure water (resistance 18.2 MΩ cm).

Samples Preparation. Aqueous solutions of PEG and PAAm with a concentration of 10% are prepared separately. Then, blends are prepared by mixing the two polymer solutions and water. Total

* Corresponding author. E-mail: tetsuharu.narita@espci.fr.

10.1021/ma071538t CCC: $37.00
Published on Web 10/13/2007

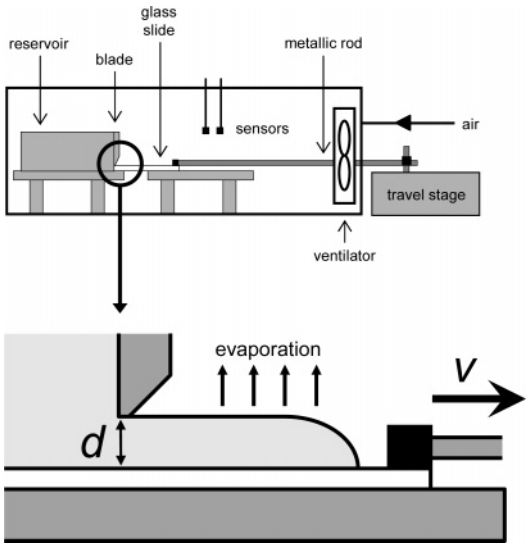

Figure 1. Experimental setup.

polymers concentration is kept 4.5%, and the mass ratios of the two polymers PEG/PAAm were 89/11, 72/28, 50/50, 28/72, and 11/89. All the initial solutions are in the one-phase region of the phase diagram.

Glass slides are used as substrates and prepared in the following way: they are washed with detergent, rinsed off successively with distilled water and ethanol, and then dried under compressed air. The contact angle of water is 5°.

We prepared polymer films on glass slides by blade coating in a conditioned chamber. Figure 1 shows the experimental setup. A reservoir of a polymer solution is equipped with a blade (Elcometer, France) in a drying chamber made of PMMA plates. A glass slide connected to a microstep travel linear stage (Newport) is put in the reservoir and then drawn from it at a constant pulling speed v (μm/s). The polymer solution is cast on the slide by means of the blade and subjected to drying. The initial thickness of the cast film d (μm) can be controlled by changing the gap between the blade and the substrate (30−1000 μm). The cast polymer film is dried in the closed chamber, equipped with a fan which ensures the homogenization and a supply of humid air of relative humidity h (%). Since the film is not always uniform close to the border (presumably due to incomplete casting in the beginning), we did not use the part at least 1 cm from the border. Otherwise, we did not observe dependence on the position or on the pulling speed at the range studied.

AFM Imaging. The surface topography was probed by AFM. We used a Nanoscope III microscope Dimension 3100 which was operated in tapping mode. The samples are scanned at a rate from 0.3 to 0.5 Hz using a cantilever tip with a force of 40 nN, modulated at 300 kHz with vertical rms amplitude of 80 nm.

Image analyses were performed by a WsXM software[14] and Igor. Roughness R (nm) is given by the formula $R = [(1/MN)\sum_{i=1}^{M}\sum_{j=1}^{N}(Z(x,y) - \bar{Z})^2]^{1/2}$ and calculated by the software WsXM, and holes size (nm) is taken equal to the length scale obtained by calculation of power spectral density (PSD).

Optical Microscope Imaging. Optical microscope imaging was performed using a Leica DMIRE2 optical microscope equipped with a Roper Scientific "Cool Snap" CCD camera.

Results and Discussion

In Figure 2, a typical trajectory of drying is indicated as the dashed line (for 89:11 PEG/PAAm blend). In order to study the effects of phase separation on the dried film morphology, the initial solution should be in the one-phase region, and the drying trajectory should cross the binary curve and enter the two-phase region. The morphology is expected to be determined by the competition between the drying dynamics and phase

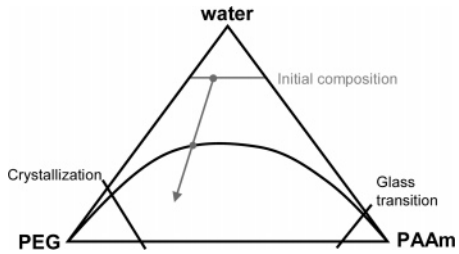

Figure 2. Schematic phase diagram for the PAAm/PEG/water system.

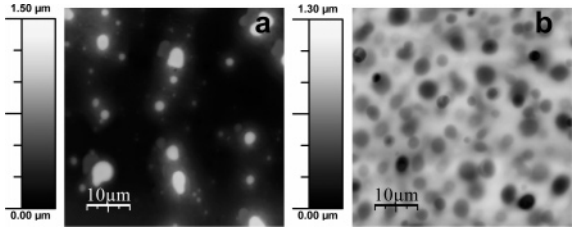

Figure 3. Surface morphology of PEG/PAAm blends (a, 11/89 and b, 89/11; $d = 50$ μm, $h = 35\%$, $T = 30$ °C) imaged by atomic force microscopy.

separation dynamics such as growth and coalescence of each phase. As the polymers concentration increases during drying, the evolution of the system will be very slow, especially by the glass transition of PAAm and the crystallization of PEG at higher concentrations.

First, we studied effects of the composition of the blend on the morphology. Single polymer solutions of PEG and PAAm, and blends of the two, are dried under the following conditions: initial thickness of the cast film $d = 50$ μm, pulling speed $v = 10$ μm/s, humidity $h = 35\%$, and temperature $T = 30$ °C.

For single polymer solutions of PAAm and PEG, since the trajectory of concentration change does not cross the binary curve and thus no phase separation is observed, the obtained dry films have a smooth surface. The roughness of the amorphous film of PAAm is 4 nm, and no particular morphology is observed. For PEG the roughness is 20 nm. This latest rough surface compared with PAAm is due to the crystallization of PEG. AFM phase imaging as well as polarizing microscopy exhibits the presence of crystalline structure.

For polymer blends, we observed two different morphologies depending on the composition. When the major component is PEG, we observed morphology consisting of mounds, protrusion of droplets from the surface. In Figure 3a, an AFM image for the 89/11 PEG/PAAm is shown. The mounds size is polydisperse with a diameter of several microns. No particular ordering is observed. The value of mean square roughness is close to 200 nm. Kumacheva et al. observed a morphology with mounds for a PS/PMMA/toluene system.[5] They showed drying rate dependence of the polydispersity of the mounds size. In our system, the fact that the PAAm is highly polydisperse in molecular weight might be influential. We did not do further study on this composition.

When the major component is PAAm (PEG/PAAm = 11/89), we observed a surface with holes (Figure 3b). Like the mounds for the 89/11 blend, these holes are polydisperse with a diameter of several micrometers, about 100 nm in depth. Some holes coalesced together. The value of mean square roughness is about 150 nm for the 11:89 PEG/PAAm blend. No particular periodicity or alignment is observed in the position of the hole. We performed the selective solvent method[15] by using acetone (good solvent for PEG, poor solvent for PAAm) and confirmed that the matrix of the 11:89 PEG/PAAm film consists of the PAAm, with holes resulting from PEG-rich droplets.

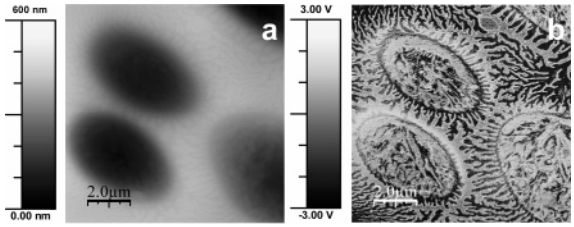

Figure 4. Surface morphology of PEG/PAAm blend (11/89, $d = 100$ μm, $h = 35\%$, $T = 25$ °C) imaged by atomic force microscopy. Topography (a) and phase imaging (b).

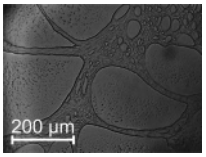

Figure 5. Surface morphology of PEG/PAAm blend (50/50, $d = 50$ μm, $h = 35\%$, $T = 30$ °C) imaged by optical microscopy.

AFM phase imaging confirms the localization of PEG at the holes. Figure 4 shows AFM images of (a) height and (b) phase for the 11/89 blend. It is clearly observed in the phase image that fingerlike branched patterns of PEG lamellar crystals are deposited on the surface of PAAm matrix from the inside of the holes to the exterior at the periphery of the holes. From the height of the image the thickness of the crystals is estimated to be less than 10 nm. Reiter and Sommer observed a similar PEG monolayer on silicon wafers.[16,17] We discuss the crystallization of PEG later in this article.

From these results one can suggest the following drying process and formation of holes. When the solvent concentration increases and reaches a critical value, phase separation occurs and droplets of PEG-rich phase appear in the PAAm-rich film from the drying surface. In the meantime, as evaporation goes on, the PAAm matrix dries and becomes glassy at the glass transition concentration. The viscosity and the elastic modulus of the matrix increase dramatically, and thus the drying kinetics of the PAAm matrix slow down. The PEG droplets which are in touch with the surface and still containing water wet the surface around the holes. The contact angle of PEG on dried PAAm is about 17°. Crystallization of PEG occurs, and the PEG-rich phase separates into PEG crystals and PEG-rich solutions whose concentration is constant. Thus, it is expected that the drying rate of the PEG-rich phase is not affected by the crystallization. In the later stages of evaporation, water finally evaporates from vitrified PAAm matrix having holes with PEG crystals leading to the final morphology.

Formation of the mounds for a film having PEG as the major component can be explained as well by the difference of drying kinetics of the two phases. When PEG is the major component, the PAAm-rich phase forms droplets. PAAm vitrifies at a certain water content. These hard glassy droplets are expected to be dried slower than the PEG-rich matrix, and finally we have a surface with mounds. The height and the bend radius of these mounds are contained respectively between 200 and 800 nm and between 5 and 10 μm.

For films containing PEG and PAAm in the ratio 50/50 and 28/72, that is to say close to the critical point of the phase diagram, optical microscopy reveals that films are made of islands and holes several hundreds micrometers large (Figure 5). AFM measurements show that both holes and islands contain themselves smaller mounds and holes.

As described for a polycarbonate/PS/THF system[18,19] or for a PEG/dextran/buffer system[9] and demonstrated by Tanaka and Araki[20] though numerical simulations, this morphology is likely to be the consequence of secondary phase separation which occurs while drying. Though the first phase separation has occurred leading to a PAAm-rich and a PEG-rich phase at a critical value, water goes on evaporating in both of them, and the equilibrium phase composition always changes. Since both phases are concentrated viscous polymer solutions, they cannot attain the quasi-equilibrium composition during drying; thus, they may undergo secondary phase separations. This entails multiscale phase separation patterns. On the contrary, when going far from the critical point, the trajectory described by the film composition when drying is closer to the phase separation curve so that the first phase separation gives equilibrium phases which do not undergo phase separation in turn.

Table 1. Summary of the Surface Morphologies Obtained for Different Blend Compositions

PEG/PAAm	morphology	crystals	roughness
100/0	smooth	yes	20
89/11	mounds	yes	180
72/28	mounds	yes	193
50/50	secondary phase separation	yes	109 for mounds
28/72	secondary phase separation	yes	110 for mounds 150 for holes
11/89	holes	yes	146
0/100	smooth	no	4

In Table 1, we summarize the obtained morphologies for different polymer blends. In the following, we focus on the 11/89 blend which exhibits a morphology containing holes and study influences of thickness and humidity on the morphology.

Polymer blends with different initial thicknesses (50, 100, 500, and 1000 μm) are dried with pulling rate, humidity, and temperature equal to 0.01 mm/s, 60%, and 31 °C.

Note that a 30 μm film dried at the same condition (humidity of 60%) exhibited dewetting of the solution from the glass substrate during drying. This phenomenon might be a consequence of destabilization of the interface by large droplets of the minor phase whose diameter is equivalent to the thickness. From the hole size observed in the AFM images, the minor phase droplets size is expected to be 2−4 μm. The final thickness of the film d_f with the initial thickness d_0 of 30 μm is estimated to be ~1.5 μm (the initial polymers concentration is 4.5%, thus $d_f \approx d_0 \times 4.5/100$), very close to the droplet radius. Studies of Wang and Composto[21] might explain the similar situation. They reported the wetting behavior of deuterated poly(methyl methacrylate) and poly(styrene-*ran*-acrylonitrile) blend films (without solvent, high temperature). They revealed different regimes of wetting and phase separation depending on the thickness: if the thickness e is really higher than R_g, the surface is enriched with PMMA and followed by a PMMA-poor layer, whereas when the thickness is under $150R_g$, droplets of SAN are encapsulated in PMMA-rich layers via different mechanisms following the range of thickness. The first step is the formation of a trilayer PMMA−SAN−PMMA followed either by lateral phase coarsening and rupture of the middle layer or by the formation of holes in the SAN-rich layer.

AFM images of surface morphology of the films of different initial thicknesses are shown in Figure 6. For all the films, we found a similar morphology with polydisperse holes without any specific orientation. No significant effect of thickness on morphology is found at the studied condition. The roughness is about 250 nm, while the hole depth is estimated to be 200−300 nm, and the lateral hole size is 3 μm; a typical profile line is shown in Figure 7. Those for homopolymer films are also shown for comparison. The large value of the mean square

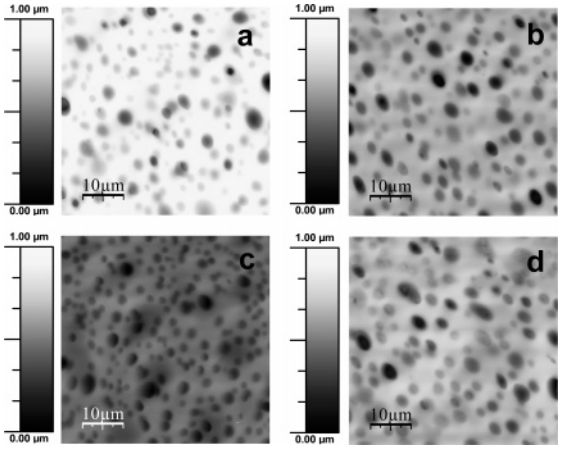

Figure 6. Surface morphology of blend 11/89 at different initial thicknesses: (a) 50, (b) 100, (c) 500,and (d) 1000 μm dried at h = 60% and T = 35 °C.

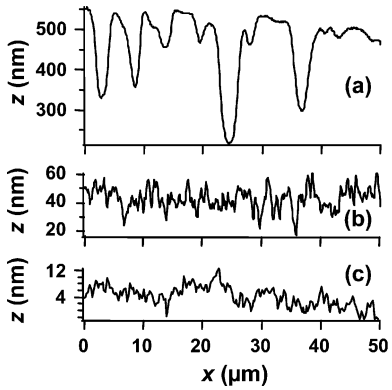

Figure 7. Line profiles of height for (a) blend 11/89, (b) PEG and (c) PAAm. d = 100 μm, h = 60%, T = 35 °C.

roughness observed for PEG homopolymer film (b) might be due to the relatively high initial thickness (50 μm) and high drying rate at 35% humidity.

The obvious constancy of morphology with thickness may be explained by heterogeneous drying of the films. When a glassy polymer solution cast is dried, the solvent evaporates from the drying surface and the local concentration of the polymer increases.[22] The evaporation rate is a parameter of this process. The evaporation creates a concentration gradient, and it is homogenized by diffusion of the solvent and polymer in the cast. This process is determined by the diffusion coefficient and thickness. When the evaporation rate is sufficiently high compared with homogenization by diffusion, a glassy skin can be formed on the surface at the glass transition concentration, and the surface morphology is fixed. Thus, the surface morphology is likely to depend only on the drying parameters such as humidity but less on thickness. In fact, we have the same result for films dried at a humidity of 35%: the roughness and hole size do not show any specific tendency on the thickness at the same thickness range studied.

Imaging by optical microscopy both from the top (drying surface side) and from the bottom (glass substrate side) shows structures due to droplets distributed heterogeneously in the film. Figure 8a,b shows the images for 11/89 PEG/PAAm blend films (50 μm) dried at h = 35%. One can see that top and bottom morphologies are different: at the bottom, larger length scale is observed. This is due to the segmentation and coalescence of the droplets observed in the literature.[9] The preferential absorption of one component on the substrate was previously reported (polyvinylpyridine/polystyrene/ethylbenzene on mica substrate).[8] In our system, both polymers are hydrophilic and there is presumably no strong preferential interaction. (The contact angle of 10% PAAm solution on glass is 43°, while that for PEG is 49°.)

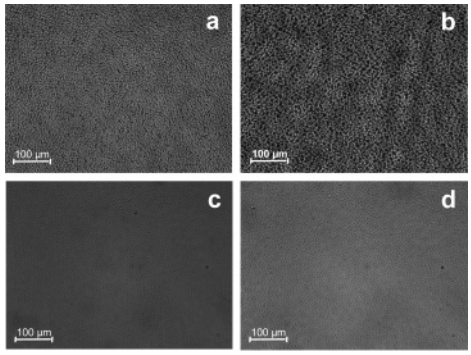

Figure 8. Top and bottom morphologies of PEG/PAAm blend (11/89) with a thickness of 50 μm at h = 35%, T = 32 °C (a, top; b, bottom) and h = 84%, T = 30 °C (c, top; d, bottom) imaged by optical microscopy.

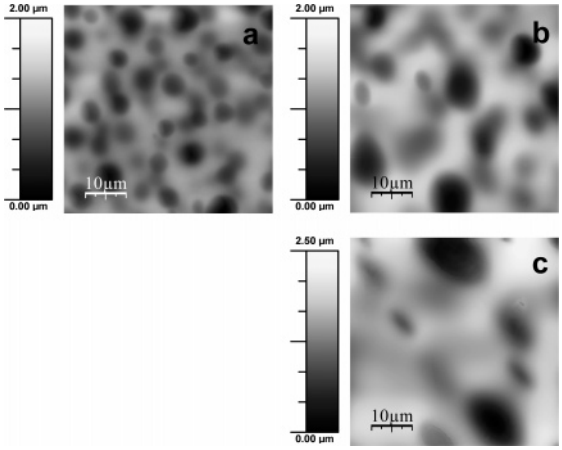

Figure 9. Surface morphology of blend 11/89 at different initial thicknesses: (a) 100, (b) 500, and (c) 1000 μm dried at h = 84% and T = 30 °C.

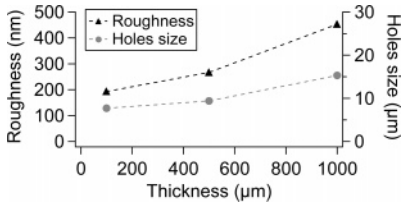

Figure 10. Variation of roughness and holes size of blend 11/89 with thickness at h = 84% and T = 30 °C.

Now, when performing this experiment at higher humidity, the result is expected to be different. We made the same experiment at a humidity of 84%, and one can clearly see the thickness dependence. As shown in Figures 9 and 10, both the roughness of the sample and the size of the holes increase with increase in the thickness. At high humidity, as the evaporation of water is slow, the water content in the cast remains high enough to keep the matrix wet and thus plasticized. Therefore, no glassy thin skin is formed and the drying is homogeneous, and for the thick film such as 1 mm, PEG-rich droplets grow and coalesce to increase in roughness and holes size. In this case, optical microscopy reveals that the bottom morphology is completely similar to the top morphology, as shown in Figure 8c,d.

What morphology do we obtain when we dry films further slower? In order to study the effect of very slow drying at high

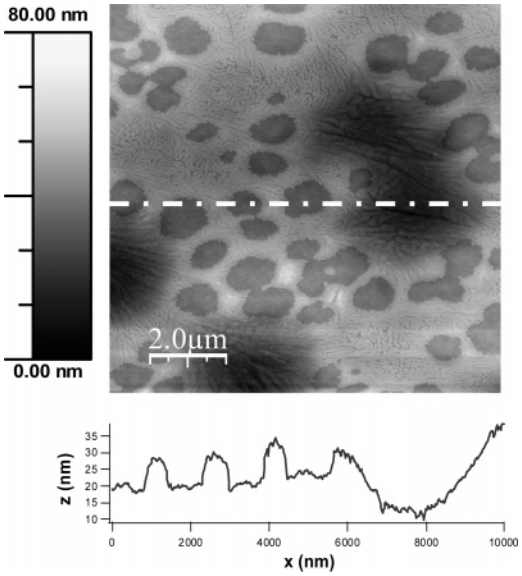

Figure 11. Surface morphology and line profile of blend 11/89 (d = 50 μm) dried at h = 99% and T = 35 °C.

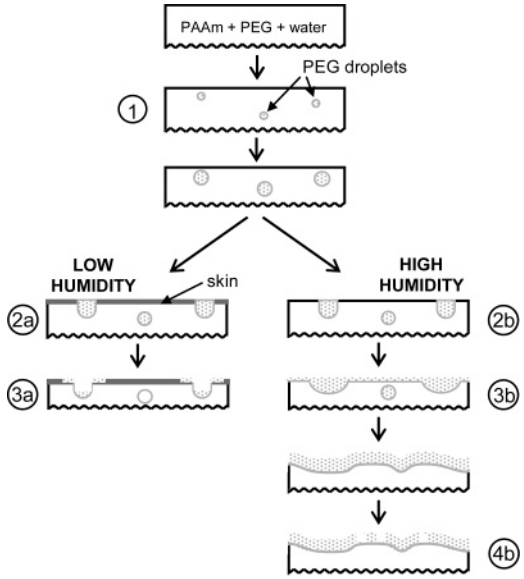

Figure 12. Schematic representation of drying process. (1) Phase separation: growth of PEG droplets and drying of PAAm matrix. For low humidity: (2a) formation of the skin and (3a) holes formation and crystallization of PEG. For high humidity: (2b) wetting by PEG, (3b) smoothing of the surface, and (4b) crystallization of PEG.

humidity on the increase in the roughness and hole size, we dried a 11/89 PEG/PAAm film very slowly under h = 99%. Figure 11 shows an AFM image of the obtained dry film with particular morphology. We found a similar morphology with holes whose lateral size is about 2 μm; however, the depth is lower: it is estimated to be 20 nm. And the roughness of the surface is also low (40 nm) compared with the films dried at lower humidity. One can see another structure: the surface has smaller holes of irregular lateral size (on the order of 1 μm). As shown in the line profile (Figure 11b), the depth of the defaults is 10 nm and uniform throughout the surface, suggesting that the film surface is covered by a monolayer of PEG crystal.

We attribute this morphology to formation of a surface-active PEG-rich phase layer at the surface as a consequence of droplets coalescence. We suggest the following mechanism of formation of this smooth surface with crystal layer. During drying, droplets of the PEG-rich phase appear close to the drying surface of the liquid film by phase separation. The droplet size increases with time due to nucleation growth and coalescence of the droplets. Since the drying is very slow at high humidity, the growth of the droplets close to the surface results in covering the surface with the PEG-rich phase because of its low surface energy. Smoothing of the surface may take place as the PAAm-rich matrix is not enough dried to be vitrified. Finally, the PAAm matrix vitrifies and the PEG-rich phase layer crystallizes. In fact, we obtained a similar structure by drying a PEG solution cast on a PAAm dry film.

Defects in the crystal layer on the surface might be attributed to the growth of the crystals from the nuclei. As previously indicated, nucleation does not occur if the films are thinner than 10−15 nm.[23] Thus, in our experiments nucleation starts from the droplets of PEG in the holes. As shown in Figures 4b and 10, we always have crystals in the holes. The fingerlike patterns develop from the holes by diffusion of amorphous PEG layer toward the growing surface of the crystals.

In our experiments, the crystal thickness did not strongly depend on the humidity or initial thickness of the PEG/PAAm blend films. PEG forms folded-chain lamellar crystals, and the crystal thickness increases with increase in the stability of the crystal. Following the estimation of the number of folds reported in the literature,[24] we estimate that the chains are folded 22 times to have 10 nm thick crystals, from the molecular weight of PEG, with assumption of regular folding of whole chains. Zhai et al.[24] reported that relatively low molecular weight PEG (5000 g/mol) can be folded much less at lower temperature close to the melting point. They reported also that annealing at a temperature below melting point results in a thickening of crystals, induced by melting and recrystallizing. We did not observe thicker crystals than 10 nm even by slow drying at 99% humidity, presumably because we used PEG with higher molecular weight (35 000 g/mol) and because the crystallization is forced by evaporation of water and thus too fast to have thicker crystals. Further studies such as time-resolved WAXS/SAXS experiments for PEG of various molecular weights are required to understand the crystallization of PEG on a polymer matrix during drying.

Conclusion

We studied the morphology of blend films of PEG/PAAm/water induced by drying and phase separation. In summary, depending on the initial composition of blend, drying of polymer leads to morphologies consisting in holes (PEG as minor phase) or in mounds (PEG as major phase). When the composition is 50/50 (and 28/72), complex multiscale surface morphologies having both holes and mounds due to secondary phase separation are observed.

The study of a PEG/PAAm blend with a 11/89 ratio reveals that the morphology depends on the drying rate. We found two regimes described in Figure 12. When the film dries quickly at low humidity, the drying is heterogeneous in the direction of thickness and a glassy skin is formed at the surface. This skin may fix the surface structure, and the morphology is less dependent on the thickness. PEG crystal monolayers with fingerlike patterns are found in the holes and their periphery, suggesting diffusion of PEG chains from the nuclei in the holes. Increasing the humidity increases the time for PEG-rich droplets to evolve by coalescence, and thus the roughness and hole size increase. When the film dried very slowly at very high humidity, the surface of the film is covered by the PEG-rich phase layer as a consequence of the coalescence and due to its low surface energy. The PAAm-rich matrix may be smoothened by the

interfacial tension, and the surface is covered by the PEG crystals.

This system could be a model to study the crystallization in restricted geometries by controlling the film thickness and droplet size. The observed pattern formation might attract applications in the biomaterial field by replacing PAAm with biocompatible polymers.

Acknowledgment. This work was partly funded by the grant DEPSEC of the Agence Nationale de la Recherche, France.

References and Notes

(1) Gutmann, J. S.; Müller-Buschbaum, P.; Stamm, M. *Faraday Discuss.* **1999**, *112*, 286−297.
(2) Müller-Buschbaum, P.; Gutmann, J. S.; Wolkenhauer, M.; Kraus, J.; Stamm, M.; Smilgies, D.; Petry, W. *Macromolecules* **2001**, *34*, 1369−1375.
(3) Walheim, S.; Böltau, M.; Mlynek, J.; Krausch, G.; Steiner, U. *Macromolecules* **1997**, *30*, 4995−5003.
(4) Tanaka, K.; Takahara, A.; Kajiyama, T. *Macromolecules* **1996**, *29*, 3232−3239.
(5) Kumacheva, E.; Li, L.; Winnik, M. A.; Shinozaki, D. M.; Cheng, P. C. *Langmuir* **1997**, *13*, 2483−2489.
(6) Li, L.; Sosnowski, S.; Chaffey, C. E.; Balke, S. T.; Winnik, M. A. *Langmuir* **1994**, *10*, 2836−2841.
(7) Dalnoki-Veress, K.; Forrest, J. A.; Stevens, J. R.; Dutcher, J. R. *J. Polym. Sci., Part B: Polym. Phys.* **1996**, *34*, 3017−3024.
(8) Cui, L.; Han, Y. *Langmuir* **2005**, *21*, 11085−11091.
(9) Hopkinson, I.; Myatt, M. *Macromolecules* **2002**, *35*, 5153−5160.
(10) Mitov, Z.; Kumacheva, E. *Phys. Rev. Lett.* **1998**, *81*, 3427−3430.
(11) Saraf, R. F.; Ostrander, S.; Feenstra, R. M. *Langmuir* **1998**, *14*, 483−489.
(12) Mishra, R.; Rao, K. J. *Eur. Polym. J.* **1999**, *35*, 1883−1894.
(13) Taden, A.; Landfester, K. *Macromolecules* **2003**, *36*, 4037−4041.
(14) Horcas, I.; Fernandez, R.; Gomez-Rodriguez, J. M.; Colchero, J.; Gomez-Herrero, J.; Baro, A. M. *Rev. Sci. Instrum.* **2007**, *78*, 013705.
(15) The surface of the sample is rinsed out with acetone (a good solvent for PEG and a poor solvent for PAAm) for 1 min. About 100 mL of acetone was used, which is enough to remove a 25 μm PEG film of a glass substrate. After treatment the surface morphology with holes remains intact.
(16) Reiter, G.; Sommer, J. U. *Phys. Rev. Lett.* **1998**, *80*, 3771−3774.
(17) Reiter, G.; Sommer, J. U. *J. Chem. Phys.* **2000**, *112*, 4376−4383.
(18) Yamamura, M.; Nishio, T.; Kajiwara, T.; Adachi, K. *Chem. Eng. Sci.* **2002**, *57*, 2901−2905.
(19) Yamamura, M.; Mikuriya, T.; Kajiwara, T.; Adachi, K. *Ind. Eng. Chem. Res.* **2002**, *41*, 4409−4413.
(20) Tanaka, H.; Araki, T. *Phys. Rev. Lett.* **1998**, *81*, 389−392.
(21) Wang, H.; Composto, R. J. *Interface Sci.* **2003**, *11*, 237−248.
(22) Romdhane, I. J.; Price, P. E.; Miller, C. A.; Benson, C. T.; Wang, S. *Ind. Eng. Chem. Res.* **2001**, *40*, 3065−3075.
(23) Despotopoulou, M. M.; Frank, C. W.; Miller, R. D.; Rabolt, J. F. *Macromolecules* **1996**, *29*, 5797.
(24) Zhai, X. M.; Wang, W.; Ma, Z. P.; Wen, X. J.; Yuan, F.; Tang, X. F.; He, B. L. *Macromolecules* **2005**, *38*, 1717−1722.

MA071538T